Integrated and Sustainable Preparation of Functional Nanocellulose via Formic Acid/Choline Chloride Solvents Pretreatment

Meiyan Wu
Qingdao Institute of BioEnergy and Bioprocess Technology Chinese Academy of Sciences
Keyu Liao
Qingdao Institute of BioEnergy and Bioprocess Technology Chinese Academy of Sciences
Chao Liu
Qingdao Institute of BioEnergy and Bioprocess Technology Chinese Academy of Sciences
Guang Yu
Qingdao Institute of BioEnergy and Bioprocess Technology Chinese Academy of Sciences
Mehdi Rahmaninia
Tarbiat Modares University
Haiming Li
Dalian Polytechnic University
Bin Li (libin@qibebt.ac.cn)
Qingdao Institute of BioEnergy and Bioprocess Technology Chinese Academy of Sciences
https://orcid.org/0000-0002-8903-3874

Research Article

Keywords: nanocellulose, deep eutectic solvent, formic acid, ball milling, comparison, Pickering emulsion

Posted Date: July 6th, 2021

DOI: https://doi.org/10.21203/rs.3.rs-627809/v1

Abstract

Formic acid/choline chloride (F-DES), one of high-efficiency deep eutectic solvents (DES) for lignocellulose pretreatment, has great potential in the production of nanocellulose (NC). In this work, the integrated preparation of cellulose nanocrystals (CNCs) and cellulose nanofibrils (CNFs) was developed using F-DES pretreatment and the followed ball milling. Then, the properties of the resultant NC products (F-NC) were comprehensively investigated. The NC samples obtained from direct ball milling and urea/choline chloride (U-DES) plus ball milling (i.e. B-NC, and U-NC, accordingly) were used for comparison. Characterization results showed that similar to U-DES, F-DES pretreatment could effectively enhance the fibrillation of cellulose and facilitate the followed ball milling for the production of NC, and the yields of NC (CNCs plus CNFs) were over 95%. Yet, compared with B-NC and U-NC, F-NC with surface ester groups had better ability to stabilize the oil/water interface for further preparation of oil-in-water Pickering emulsion. In addition, F-DES has lower viscosity than U-DES. The recovery rate of F-DES could reach 92% after three cycles, and the recycled F-DES without obvious increase of viscosity showed better reusability to make the whole process clean and sustainable.

Introduction

Cellulose with the structure of β-1, 4 linked D-glucose units is an abundant, sustainable and renewable resources (Yang et al. 2021). Researchers have been working on the application of cellulose and cellulose derivatives in various fields, such as membrane materials (Wu et al. 2020), packaging materials (Ferrer et al. 2017) and gel materials (Ajdary et al. 2020). In recent years, nanocellulose (NC) as a nano-sized cellulosic material has attracted great attention due to its unique physicochemical properties (e.g. nanometer scale, high specific surface area, excellent mechanical properties) (Pires et al. 2019). NC derived from the “Top down” method, mainly including rod-like cellulose nanocrystals (CNCs) and noodle-like cellulose nanofibrils (CNFs), is prepared from lignocellulose using direct chemical/mechanical treatment or chemical/enzymatic pretreatment plus post-mechanical treatment (Dufresne 2020). Generally, direct mechanical treatment method of lignocellulose requires high energy consumption (Zhang et al. 2015), and direct chemical/enzyme treatment usually needs harsh conditions (e.g. high acid concentration) or long hydrolysis time (Pääkkö et al. 2007; Tang et al. 2011). Thus, chemical pretreatment plus post-mechanical treatment is a commonly used method to prepare NC.

As known, chemical pretreatment methods mainly refer to acid hydrolysis (Bian et al. 2017), oxidation treatment (Liu et al. 2016), ionic liquid treatment (Man et al. 2011), supercritical hydrolysis (Novo et al. 2015), *etc*. However, these methods often involve toxic, corrosive and expensive chemicals, high process cost, or chemical recovery problems (Novo et al. 2015; Tomé et al. 2018). In recent years, deep eutectic solvents (DES) treatment were used as a green and sustainable method for the biorefinery of lignocelluloses or the preparation of NC materials. DES with the low melting point could be simply prepared by mixing hydrogen bond donor molecule and hydrogen acceptor molecule (Abbott et al. 2001), and easily recycled by phase separation and evaporation of water (Loow et al. 2017). DES also exhibited good removal ability of hemicellulose and lignin from lignocellulose due to their excellent dissolving

capacity (Liu et al. 2017). According to the previous reports, various DES, such as oxalic acid/choline chloride (Yang et al. 2019), urea/choline chloride (Laitinen et al. 2017b), glycerol/aminoguanidine hydrochloride (Li et al. 2018), urea/guanidine hydrochloride (Li et al. 2017), urea/sulfamic acid (Lynam et al. 2017), urea/lithium chloride (Selkala et al. 2016) and imidazole/triethylmethylammonium chloride (Sirviö and Visanko 2017; Sirvio 2018), were employed as high-efficient pretreatment solvents to prepare NC. These preparation methods and products are summarized in Tab. S1. Among them, urea/choline chloride (U-DES) pretreatment as a commonly used approach can facilitate the swelling of cellulose fibers without the dissolution and chemical structure damage of cellulose (Zhang et al. 2012).

Moreover, formic acid is a good hydrogen bond donor, which can mix with choline chloride to produce a new-type DES (F-DES) (Lynam et al. 2017). In previous work, the integrated production of NC (CNCs and CNFs) with tailored characteristics was achieved via formic acid hydrolysis plus the followed homogenization, and formic acid was readily recycled by vacuum distillation due to its low boiling point (100.8 ºC) (Lv et al. 2019). The integrated preparation of NC (CNCs + CNFs) could get a high yield of NC and reduce the production cost (Chen et al. 2016; Wang et al. 2017). However, F-DES pretreatment has only been reported for the component fractionation/pretreatment of lignocellulose to promote enzymatic saccharification (Lynam et al. 2017), and there is no report regarding the F-DES pretreatment for the integrated production of NC.

In addition, there were many mechanical treatment methods for preparing NC (Tab. S1). Especially, ball milling with relatively low process cost may be a suitable way for mechanical treatment without any congestion (Piras et al. 2019; Yu et al. 2019). Cellulose feedstock can be fully pulverized, mixed and homogenized under the intense friction and impact energy from the grinding balls (Karinkanta et al. 2014). Therefore, F-DES pretreatment plus ball milling post-treatment may have great potential application in the integrated preparation of NC.

Hence, in this work, we put forward an integrated method of F-DES (formic acid/choline chloride) pretreatment plus ball milling post-treatment in order to prepare CNCs and CNFs, and this method was compared with the most studied urea/choline chloride (U-DES) pretreatment method and direct ball milling method. Furthermore, the obtained CNCs and CNFs were comprehensively characterized for comparison, and the recovery efficiency and reusable performance of DES (F-DES and U-DES) were also investigated to make the whole process clean and sustainable. In addition, the NC samples with different characteristics to stabilize the oil/water interface were also investigated for the preparation of oil-in-water Pickering emulsion. The biodegradable and nontoxic Pickering emulsion using nanocellulose may have great potential to produce food, beverage, cosmetics, medicine, *etc*.

Experimental

Materials

Microcrystalline cellulose (MCC, particle size ≤ 50 μm) from Aladdin Reagents (Shanghai, China) was used as raw cellulose materials. Choline chloride (99 wt%) was obtained from Henan Xingyuan Chemicals Co., Ltd. (China). Urea (99 wt%), formic acid (88 wt%) and other reagents were purchased from Sinopharm Chemical Reagent Co., Ltd. (China). All chemicals were directly used without any further purification.

Preparation method of nanocellulose samples

F-DES was prepared by mixing choline chloride and formic acid with the molar ratio of 1:2 in a round-bottom flask under 150 rpm stirring at room temperature (25 ºC) for 30 min, then a clear liquid of F-DES was obtained. For comparison, U-DES was also prepared by mixing choline chloride and urea with the molar ratio of 1:2, and the liquid of U-DES was obtained after heated to 90 ºC under 150 rpm stirring for 30 min in an oil bath. Then, MCC was added in F-DES and U-DES with the fiber consistency of 5 wt%, respectively. The reaction was taken place in an oil bath at 90 ºC for a certain time. After that, the dispersion was centrifuged with the centrifugal force of 11,000 g for 5 min to separate the supernatant and solid residue. The solid residue was washed five times by centrifugation with 1000 *g* of deionized (DI) water and then the pretreated MCC samples were obtained. The pretreated MCC with F-DES and U-DES were named as F-MCC and U-MCC, respectively. The supernatant was efficiently collected by rotary evaporation at 60 ºC until there was no mass change of the liquid, and then the recycled F-DES and U-DES were obtained for reuse. F-DES recycled after the first, second and third cycle were named as F-DES (R1), F-DES (R2) and F-DES (R3), respectively, and U-DES recycled after the first, second and third cycle were named as U-DES (R1), U-DES (R2) and U-DES (R3), respectively.

The recovery rates of the recycled F-DES and U-DES were calculated according to the formula (1).

$$\text{Recovery rate (\%)} = m_2/m_1 \times 100\% \qquad (1)$$

Wherein, m_1 (g) is the mass of the initial DES, and m_2 (g) is the mass of the recycled DES by rotary evaporation.

Afterwards, the pretreated MCC with a solid content of 25% in DI water was put into the ball milling tank containing zirconia beads, and the mass ratio of bead and MCC sample was 40:1. The sample was milled using a Planetary Ball Mill (DECO, PBM-AD-0.4L, China) with a speed of 300 rpm for a certain time. In addition, MCC was directly ball milled with the same procedure as control. The resultant NC were collected by adding 500 g of DI water, and then centrifuged with a centrifugal force of 5000 *g* for 5 min to separate the CNCs and CNFs (CNCs with more dispersion stability could not be precipitated under this centrifugation). All the abbreviations in this work are listed in Tab. S2, and the integrated preparation route of NC is shown in Fig. 1. The yield of NC samples was calculated according to the formula (2).

$$\text{Yield (\%)} = m_4/m_3 \times 100\% \qquad (2)$$

Wherein, m_3 (g) is the dry mass of the initial MCC, and m_4 (g) is the dry mass of the resultant NC (CNCs or CNFs).

Characterization

The Crystallinity Index (*CrI*) of the pretreated MCC powder (F-MCC and U-MCC) and the resultant NC powder was tested by an X-ray diffractometer (Bruker, D8 ADVANCE, Germany). The Ni-filtered Cu Kα radiation was generated at 80 mA and 40 kV. The range of scattering angle (2θ) was from 10 to 40º with a scanning speed of 0.5 º/min. The *CrI* of all samples was calculated based on the formula (3) with the subtraction of the test background.

$$CrI = (I_{200} - I_{am})/I_{200} \quad (3)$$

Wherein, I_{200} is the maximum intensity of the diffraction from the peak (200), and I_{am} is the minimum intensity of the diffraction between 101 and 200 peaks (Du et al. 2016a).

Fourier Transform Infrared Spectroscopy (FTIR) spectra of the samples were recorded on a spectrometer (Thermo Fisher, Nicolet 6700, USA) using the KBr pellet method and the wavenumber of spectra ranged from 4000 to 500 cm^{-1}. The surface morphologies of the freeze-dried samples were imaged by a Scanning Electron Microscope (SEM, Hitachi S-4800, Japan). The images of NC morphologies were obtained via a Transmission Electron Microscope (TEM, Hitachi H-7600, Japan). The TEM samples were prepared by dropping NC suspension with a consistency of 0.01 wt% on the copper network. When the droplet was air-dried at room temperature, the sample was stained with 2 wt% uranyl acetate solution for 30 min, and then the stained samples was dried at room temperature. The mean diameters of NC samples were calculated using the Nano measurer software. NC suspensions with the consistency of 0.01 wt% were treated by ultrasonication (200 W, 40 kHz) for 30 s, and then the equivalent volume size and Zeta potential of NC suspensions were immediately tested using a Particle Size Analyzer (NanoBrook, 90Plus, USA), and the transmittance of NC suspensions was tested by a UV-Vis spectrophotometer (Hitachi, U-4100, Japan) with the wavenumber from 350 to 800 nm. The thermal stability of various samples was investigated using a thermal analyzer (Netzsch, STA449F5 jupiter, USA) from 50 to 600 ºC with a heating rate of 5 ºC/min under N_2 gas. The onset temperature of thermal degradation (T_{on}) was obtained using the tangent method (He et al. 2019). Moreover, the viscosity of DES and the recycled DES samples was measured by a Viscosity Tester (PerkinElmer, RVA-TecMaster, Sweden), and the CNCs and CNFs samples were prepared through the same procedure using the recycled DES to investigate the pretreatment effectiveness on MCC. In addition, the CNCs and CNFs from B-NC2, U-NC2 or F-NC2 were added in the oil/water mixture containing 10 wt% oleic acid and 90 wt% DI water to discuss the ability to stabilize the oil/water interface, and the amount of CNCs or CNFs in the mixture was 0.2 wt%. Here, oleic acid was dyed by adding 0.01 wt% oil red for better observation. After ultrasonication (200 W, 40 kHz) for 90 s, the oil/water mixture was imaged by an optical microscope (Olympus, BX-4, Japan) with 20× or 40× objective. The droplet size in Pickering emulsion was calculated using the Nano measurer software. The F-NC film was prepared by vacuum filtration of F-NC suspension with a

consistency of 0.1%, and then dried in an oven at 50 ºC for 5 h. The water contact angle of film was tested using a contact angle goniometer (KINO, SL200B, USA) at ambient temperature.

Results And Discussion

Effect of DES pretreatment on MCC

As mentioned, MCC was firstly pretreated using F-DES and U-DES for a certain time, respectively, and then ball milled to prepare NC (CNCs and CNFs). Here, F-MCC and U-MCC after ball milling for 8 or 16 h were accordingly named as F-NC1 and U-NC1, or F-NC2 and U-NC2, respectively. Similarly, MCC after direct ball milling for 8 or 16 h was marked as B-NC1 or B-NC2, respectively. CNCs and CNFs in NC samples were also named accordingly, such as F-CNCs1 and F-CNFs1 in F-NC1. All the abbreviations in this work are listed in Tab. S2, and the integrated preparation route of NC is shown in Fig. 1.

The digital images of the obtained DES (F-DES and U-DES) and the corresponding pretreated MCC (F-MCC and U-MCC) are shown in Fig. S1 and S2, respectively. Compared with MCC, F-MCC and U-MCC samples after DES pretreatment for 2 h showed the same crystal structure of cellulose I with the typical peaks of 14.8 º (1–10), 16.5 º (110), 20.4 º (012), 22.6 º (200), and 34.4 º (004) in the XRD patterns (Fig. 2a). This phenomenon indicated that MCC treated by F-DES and U-DES had no change on crystal structure of cellulose (Ling et al. 2018). Moreover, the crystallinity index (*CrI*) of U-MCC remained steady basically after U-DES pretreatment for 3 h and then decreased with the further prolonged pretreatment time, while the *CrI* of F-MCC decreased after F-DES pretreatment for 3 h (Fig. S3). Further increasing of DES pretreatment time caused the damage of crystalline regions of cellulose, thus resulting in a clear decrease of *CrI* (Suopajarvi et al. 2017). According to the previous reports, the degraded cellulose could cause the increase of the viscosity of DES, which limited the further recycling and utilization of DES. For this reason, DES pretreatment time of 2 h without the clear change of *CrI* was employed for the subsequent experiments.

Moreover, the chemical structure of MCC before and after DES pretreatment for 2 h was also studied by FTIR spectra (Fig. 2b). In the spectra of all cellulose samples, there are two peaks at 3342 and 2899 cm^{-1} assigning to O-H bonds and C-H bonds in the cellulose chain, and the peaks appearing at 1644 and 1430 cm^{-1} are attributed to O-H bonds from water and C-H bonds, respectively (Wu et al. 2020). Specially, compared with MCC and U-MCC, an absorption peak at 1720 cm^{-1} is shown in the spectrum of F-MCC, which belongs to the newly formed ester groups (Zhang et al. 2021). According to previous study, esterification reaction between cellulose and formic acid could happen in the process of formic acid pretreatment (Du et al. 2016b). As a result, the chemical structure of F-MCC is different from MCC and U-MCC, leading to the special properties of the obtained F-NC, which will be discussed in the following part.

In addition, the morphologies of MCC, U-MCC and F-MCC are shown in Fig. 2c. The surface of MCC without DES pretreatment was relative smooth and compact, while U-MCC and F-MCC after pretreatment for 2 h exhibited the disintegrated fiber with the decrease of particle size (particularly for the F-MCC

sample). These results indicated that MCC was swelled and fibrillated during U-DES and F-DES pretreatment, which was helpful for the post-mechanical treatment to product NC. This result was consistent with the effect of DES on cellulose described by Tenhunen *et al* (Tenhunen et al. 2017; Tenhunen 2016).

Effect of ball milling time on MCC

After DES pretreatment for 2 h, the obtained F-MCC and U-MCC were milled to prepare NC, and then the NC samples (B-NC, F-NC, U-NC) made from MCC, F-MCC and U-MCC were centrifuged to separate the corresponding CNCs and CNFs. In this process, ball milling time was a very important factor to influence the properties and yield of NC. With the increase of ball milling time, the fibers bundles were gradually peeled off and separated into nanofibrils under the friction actions of ball beads (Zhang et al. 2015). Thus, MCC and U-MCC suspensions became more and more homogeneous, while F-MCC with ester groups were gradually precipitated off in 2 h (Fig. S4-S6), and the corresponding CNCs and CNFs were gradually formed. As shown in TEM images (Fig. S7), the corresponding CNCs and CNFs separated from B-NC1, F-NC1 and U-NC1 suspensions were obtained after ball milling for 8 h. However, large nanofiber aggregations could still be observed in the images of all NC samples. After ball milling for 16 h, the dimensions of nanofiber aggregations of all CNCs and CNFs samples obviously decreased (Fig. 3), and the corresponding diameter was mainly around 6–18 nm (Fig. S8). Specially, the mean diameters of CNCs and CNFs from B-NC2 were 9.3 and 14.3 nm, respectively, which were larger than that from U-NC2 (9.2 and 11.7 nm) and F-NC2 (8.3 and 10.6 nm). This result also showed that U-DES and F-DES pretreatment on MCC, especially F-DES pretreatment, could facilitate to break fiber aggregation and generate NC in ball milling process.

Moreover, the equivalent volume size of MCC samples after ball milling was used to roughly evaluate the dimensions of fiber aggregation. As can be seen in Fig. S9, the equivalent volume size of B-MCC and U-MCC exhibited a sharp decrease in the beginning of ball milling, and then a slight decrease from 2 to 16 h of ball milling was observed. Furthermore, the equivalent volume size of U-MCC was smaller than that of B-MCC because U-DES pretreatment could promote the fibrillation effect of ball milling. In addition, it was worth mentioning that the equivalent volume size of F-MCC failed to be obtained using dynamic light scattering (DLS) method due to the influence of introduced ester groups on the structure of F-MCC. Hydrophobic ester groups could lead to the flocculation of cellulose in water (Du et al. 2016b), and then produce a large number of irregular floccules over the test range of the equipment. Also, as shown in the bottom-right corner of Fig. 3, CNCs and CNFs from MCC and U-MCC exhibited better dispersibility in DI water after standing for 24 h, while CNCs and CNFs from F-MCC were completely precipitated due to its hydrophobic ester groups on the surface (Du et al. 2016a). Additionally, although the resultant CNCs and CNFs from F-MCC had poor dispersion in water, they could be well dispersed in N, N-dimethylacetamide (DMAc) and dimethyl sulfoxide (DMSO) for over three months (Fig. S10). Therefore, it is easier to obtain NC with smaller size using pretreated MCC compared to the raw MCC under the same time of ball milling. In other words, F-DES and U-DES pretreatment can efficiently reduce the time of ball milling and then save the energy consumption in the process for the preparation of NC.

Properties of the obtained nanocellulose

The properties of the obtained CNCs and CNFs samples, such as Zeta potential, *CrI*, thermal stability and transmittance of NC dispersion were studied in this part. As shown in Fig. 4a, Zeta potential values of all MCC samples decreased with the increasing of ball milling time at the pH value of 7. Here, all MCC samples exhibited negatively charged property in water, and Zeta potential values of all MCC samples significantly decreased in the beginning and then remained steady during milling (Seta et al. 2020). Specially, the Zeta potential value of U-MCC was lower than that of MCC and F-MCC. This was because U-DES pretreatment was helpful for deconstruction of cellulose fibers, and thus more charged groups were exposure on the surface of sample. Moreover, the Zeta potential value of F-MCC was higher than that of MCC and U-MCC due to the formation of the uncharged ester groups on its surface (Abitbol et al. 2018).

Furthermore, F-MCC with hydrophobic ester groups had poor stability in water, but it had good stability in DMAc or DMSO. The dispersion stability of NC suspension in water can also be indicated by the transmittances of NC dispersions (Fig. 4b), because the transmittances of the NC samples in aqueous solution were related to the dispersibility and particle size (Huang et al. 2020). All NC aqueous dispersions with the consistency of 0.01 wt% exhibited good light transmittance in the visible light range from 400 to 760 nm. Especially, the transmittances of NC samples after ball milling for 16 h (B-NC2, U-NC2 and F-NC2) were lower than that of NC samples after ball milling for 8 h (B-NC1, U-NC1 and F-NC1) owing to the reduced particle size and the increased hydroxyl groups on cellulose surface after long-time mechanical processing (Sirvio et al. 2016), which can also be observed in Fig. S4-S6. In addition, the transmittances of B-NC2 and U-NC2 were lower than that of F-NC2, which was because the poor dispersibility of F-NC2 in water led to the aggregations of CNCs and CNFs in F-NC2, and thus the transmittance of the supernatant of the F-NC2 suspension increased.

Also, XRD patterns and the *CrI* of NC samples are shown in Fig. 4c and 4d, respectively. It can be seen that the MCC and all NC samples conformed to the crystal form of natural cellulose Iβ (Nishiyama 2009). There was a slight amorphization effect on MCC and the pretreated MCC during ball milling process (Ago et al. 2004), and the *CrI* of B-NC1 and B-NC2 decreased by 1.8% and 4.1%, respectively, compared with MCC. Correspondingly, the *CrI* of U-NC1 and U-NC2 decreased by 6.6% and 7.5%, respectively, compared to U-MCC, and the *CrI* of F-NC1 and F-NC2 decreased by 2.8% and 5.4%, respectively, in comparison with F-MCC. The reduction of *CrI* during ball milling was because part of the crystalline region of cellulose was damaged under the friction of beads in milling (Silva et al. 2012). After DES pretreatment, the U-MCC and F-MCC with smaller particle sizes were more vulnerable to be defibrillated in ball milling compared to the initial MCC with large size and more compact structure (Fig. 2c) (Karinkanta et al. 2014). Therefore, a relatively more decrease of the *CrI* of U-MCC and F-MCC with the extension of milling time was observed in comparison with MCC.

In addition, the thermal stability of MCC and the resultant NC samples after ball milling for 16 h was further investigated using TG analysis. TG curves in Fig. 4e show that MCC and all NC samples exhibited the similar degradation trend of the weight loss, and the weight loss at 300–400 °C was related to the

decomposition of cellulose and the formation of volatile substances (Du et al. 2020). For MCC, the onset temperature of thermal degradation (T_{on}) was 367 ºC and the temperature at maximum degradation rate (T_{max}) was 383 ºC (Fig. 4e and S11). The T_{on} and T_{max} of all NC samples were lower than that of MCC because of more exposed surface as well as the smaller sizes and *CrI* values of NC samples (Wang et al. 2007). Moreover, the T_{on} of CNCs samples was higher than that of the corresponding CNFs samples due to the relative high content of crystallization zone in CNCs (Du et al. 2020). Specially, the T_{on} and T_{max} of F-CNCs2 and F-CNFs2 were all lower than that of the corresponding CNCs and CNFs in B-NC2 and U-NC2. This result was because of the smaller sizes of F-CNCs2 and F-CNFs2 resulted from formic acid hydrolysis during F-DES pretreatment (Fig. 3).

Yields of CNCs and CNFs in nanocellulose samples

The yields of NC samples and the ratio of CNCs and CNFs in NC samples are one of the most important factors particularly for the large-scale integrated production. As shown in Fig. 4f, the total yields of B-NC1 and B-NC2 samples were 97.0% and 96.4%, respectively, due to the weight loss in the process of washing. The total yields of U-NC (U-NC1 and U-NC2) samples were similar to that of B-NC, while the total yields of F-NC (F-NC1 and F-NC2) samples were decreased to 95.3% and 95.2%, respectively. This phenomenon was probably because a small amount of cellulose was hydrolyzed by formic acid during F-DES pretreatment (Lv et al. 2019). Moreover, the yields of CNCs in U-NC1 and F-NC1 were 7.1% and 7.8%, respectively, which were about 3 times higher than that of B-NC1 (2.4%). Also, the yields of CNCs in U-NC2 and F-NC2 were 9.7% and 12.6%, respectively, which were 1.3 and 1.8 times higher than that of B-NC2 (7.2%). Therefore, U-DES and F-DES pretreatment were of benefit to increase the yield of CNCs in the obtained NC samples with the same ball milling time. Moreover, in all NC samples, the yield of CNCs was increased and the yield of CNFs was decreased with the extension of ball milling time. These results indicated that part of fiber-like CNFs were turned into rod-like CNCs under the ball grinding force. Compared with the previous results about the integrated preparation of NC from the bleached eucalyptus kraft pulp, the total yields (95.2%) of CNCs and CNFs prepared using F-DES pretreatment plus ball milling were obviously higher than that (72.7%) using formic acid hydrolysis (Lv et al. 2019), and slightly lower than that (98.2%) using oxalic acid hydrolysis (Chen et al. 2016). Hence, DES pretreatment plus ball milling is a controllable method to produce CNCs and CNFs with a high total yield of NC, and the ratio of CNCs and CNFs in the obtained NC samples can be adjusted by tuning the preparation conditions.

Recovery of DES

According to the previous literatures, DES can be recycled and then reused to decrease the environmental pollution and save manufacturing cost (Yang et al. 2019). Hence, U-DES and F-DES were recycled using rotary evaporation and the reusability of DES was discussed accordingly. As shown in Fig. 5a, the recovery rates of U-DES and F-DES were over 95% after the first (R1) and second cycle (R2), and about 92% after the third cycle (R3). The reducing end groups of cellulose could react with formic acid and urea (Lv et al. 2019; Tenhunen et al. 2017), leading to a slight mass loss of F-DES and U-DES. Specially, the recovery rate of F-DES was a little lower compared to U-DES due to the volatilization of formic acid in the practical reaction and recycling process.

Furthermore, the viscosity of DES was generally between 10 to 5000 cP, which was greatly affected by temperature (Abbott et al. 2004). As shown in Fig. 5b, the viscosity of U-DES sharply decreased from 500 to 50 cP with the increasing of temperature from 30 to 95 ºC. However, the temperature only had a negligible influence on the viscosity of F-DES (0–50 cP). Moreover, there was no significant change in the color of the recycled U-DES and F-DES after the third cycle (R3), and the viscosity of U-DES and F-DES slightly increased with the increasing of cycle numbers due to the slight dissolution of saccharides during DES pretreatment (Morris et al.). Therefore, compared with U-DES, F-DES with much lower viscosity at 30–95 ºC exhibited better operational performance, which was greatly helpful to pretreat cellulose for the preparation of NC.

As reported, the high viscosity of DES could lead to the difficulties of reuse and a lower effect of pretreatment (Sirviö et al. 2019). Thus, the recycled U-DES (R3) and F-DES (R3) were reused to pretreat MCC through the same procedure, and then CNCs and CNFs samples were obtained after ball milling for 16 h. As can be seen, the mean diameter of these CNCs and CNFs prepared using the recycled DES were similar to the CNCs and CNFs prepared using fresh DES (Fig. S12). Hence, it can be regarded that the same effectiveness of U-DES/F-DES pretreatment on MCC was achieved using recycled DES after the third cycle.

The ability of CNCs or CNFs to stabilize the oil/water interface

Based on the previous reports, the CNFs are more suitable to be used as adsorbing materials, and building blocks for the preparation of functional materials (e.g. cellulose nanopaper) (Wu et al. 2020), and the CNCs are more suitable to be used as the dispersing and stabilizing agents in oil/water interface (Laitinen et al. 2017a), and strengthening agents (Chen et al. 2019), *etc.* Herein, the ability of the obtained CNCs and CNFs to stabilize the oil/water interface was investigated by producing oil-in-water Pickering emulsion. As shown in Fig. 5c, the oil (oleic acid, dyed with oil red)/water mixture (10/90, w/w) containing 0.2 wt% CNCs and CNFs samples (based on the mass of oil/water mixture) were pink and relatively homogenous after ultrasonication. After standing for 24 h, only the mixture containing F-CNCs2 was homogenous, the mixtures containing other CNCs and CNFs samples showed the obvious delamination. From the microphotograph of the oil/water mixtures (Fig. 5d), the instable droplets with different diameter were seen in the mixture containing B-CNCs2, while only the aggregations of oil or nanofibers were observed in the mixture containing B-CNFs2, U-CNCs2 and U-CNFs2. This phenomenon was because both B-NC2 and U-NC2 with better surface hydrophilicity could hardly absorb oleic acid (Fig. 3), and then failed to obtain homogenous emulsions. Interestingly, the oil/water mixture containing F-CNCs2 could form the stabilized oil-in-water Pickering emulsion with a rather narrow distribution of droplets size around 32 μm (Fig. 5d and S13), and the mixture containing F-CNFs2 could also form oil-in-water Pickering emulsion, but this emulsion was relatively instable probably because of the relatively larger size of F-CNFs2. Therefore, compared with B-NC2 and U-NC2, F-NC2 (F-CNCs2 and F-CNFs2) had better compatibility to oil in the oil/water mixture, and exhibited better ability to stabilize the oil/water interface.

This result was probably due to the suitable hydrophilicity of F-NC with hydrophilic hydroxyl groups and hydrophobic ester groups (Du et al. 2016a; Kalashnikova et al. 2012). Generally, the stability of Pickering emulsion is highly dependent on the wettability, size, and concentration of emulsifier, and it is reported that the optimal water contact angle of the emulsifier particles is 70–86º or 94–110º to form oil-in-water or water-in-oil Pickering emulsion. As tested, the water contact angle of F-NC film was about 82º, so that the resultant F-NC using F-DES (formic acid/choline chloride) pretreatment in this work could be more suitable for the preparation of oil-in-water Pickering emulsion compared to B-NC and U-NC products.

Conclusions

In this work, a new type F-DES pretreatment with the followed ball milling were first used for the integrated preparation of CNCs and CNFs, and this method was compared with commonly used U-DES pretreatment. Results showed that U-DES and F-DES pretreatment of MCC could decrease the dimensions of fiber aggregation, which was helpful to defibrillation of the followed ball milling to product NC. Compared with U-DES, F-DES with much lower viscosity exhibited better usability and pretreatment effect to obtain the F-NC with smaller diameter, and a similar recovery rate after three cycles. Moreover, the recycled F-DES (after third cycle) also exhibited comparable pretreatment effectiveness on MCC for the preparation of NC. Therefore, the F-DES pretreatment and the followed ball milling is a green, efficient, and sustainable method for the production of NC with a high yield (95%) from cellulose materials under mild conditions.

In addition, compared with B-NC and U-NC samples, the F-NC had surface ester groups, leading to a poor dispersibility in water but very good dispersibility in DMAc and DMSO. Due to the unique surface characteristics, the F-NC exhibited better ability to stabilize the oil/water interface for the preparation of oil-in-water Pickering emulsion. F-NC may also have great potential to be used as a building block in plastic/rubber systems or advanced materials.

Declarations

Acknowledgments

This work was financially supported by the National Natural Science Foundation of China (No. 31870568), Shandong Provincial Natural Science Foundation for Distinguished Young Scholar (China) (No. ZR2019JQ10), Shandong Provincial Natural Science Foundation, China (No. ZR2018BC044), the Department of Education, Liaoning Province (2018 Annual Innovative Personnel Project of Liaoning Provincial Institutions of Higher Education), and the Foundation (No. KF201802, and KF201701) of Key Laboratory of Pulp and Paper Science and Technology of Ministry of Education/Shandong Province of China.

Declaration of Competing Interest

The authors reported no declarations of interest.

References

1. Abbott AP, Boothby D, Capper G, Davies DL, Rasheed RK (2004) Deep eutectic solvents formed between choline chloride and carboxylic acids versatile alternatives to ionic liquids J Am Chem Soc 126:9142-9147 https://doi:10.1021/ja048266j
2. Abbott AP, Capper G, Davies DL, Munro HL, Rasheed RK, Tambyrajah V (2001) Preparation of novel, moisture-stable, lewis-acidic ionic liquids containing quaternary ammonium salts with functional side chains Chem Commun 19:2010-2011 https://doi:10.1039/b106357j
3. Abitbol T, Kam D, Levi-Kalisman Y, Gray DG, Shoseyov O (2018) Surface charge influence on the phase separation and viscosity of cellulose nanocrystals Langmuir 34:3925-3933 https://doi:10.1021/acs.langmuir.7b04127
4. Ago M, Endo T, Hirotsu T (2004) Crystalline transformation of native cellulose from cellulose I to cellulose ID polymorph by a ball-milling method with a specific amount of water Cellulose 11:163-167 https://doi:10.1023/B:CELL.0000025423.32330.fa
5. Ajdary R, Tardy BL, Mattos BD, Bai L, Rojas OJ (2020) Plant nanomaterials and inspiration from nature: water interactions and hierarchically structured hydrogels Adv Mater e:2001085-2001116 https://doi:10.1002/adma.202001085
6. Akartuna I, Studart AR, Tervoort E, Gonzenbach UT, Gauckler LJ (2008) Stabilization of oil-in-water emulsions by colloidal particles modified with short amphiphiles Langmuir 24:7161-7168 https://doi:10.1021/la800478g
7. Bian H, Chen L, Dai H, Zhu JY (2017) Integrated production of lignin containing cellulose nanocrystals (LCNC) and nanofibrils (LCNF) using an easily recyclable di-carboxylic acid Carbohydr Polym 167:167-176 https://doi:10.1016/j.carbpol.2017.03.050
8. Chen L, Zhu JY, Baez C, Kitin P, Elder T (2016) Highly thermal-stable and functional cellulose nanocrystals and nanofibrils produced using fully recyclable organic acids Green Chem 18:3835-3843 https://doi:10.1039/C6GC00687F
9. Chen QJ, Zhou LL, Zou JQ, Gao X (2019) The preparation and characterization of nanocomposite film reinforced by modified cellulose nanocrystals Int J Biol Macromol 132:1155-1162 https://doi:10.1016/j.ijbiomac.2019.04.063
10. Du H, Liu C, Mu X, Gong W, Lv D, Hong Y, Si C, Li B (2016a) Preparation and characterization of thermally stable cellulose nanocrystals via a sustainable approach of FeCl3-catalyzed formic acid hydrolysis Cellulose 23:2389-2407 https://doi:10.1007/s10570-016-0963-5
11. Du H, Liu C, Zhang Y, Yu G, Si C, Li B (2016b) Preparation and characterization of functional cellulose nanofibrils via formic acid hydrolysis pretreatment and the followed high-pressure homogenization Ind Crop Prod 94:736-745 https://doi:10.1016/j.indcrop.2016.09.059
12. Du H, Parit M, Wu M, Che X, Wang Y, Zhang M, Wang R, Zhang X, Jiang Z, Li B (2020) Sustainable valorization of paper mill sludge into cellulose nanofibrils and cellulose nanopaper J Hazard Mater 400:123106-123116 https://doi:10.1016/j.jhazmat.2020.123106

13. Dufresne A (2020) Preparation and properties of cellulose nanomaterials Paper and Biomaterials 5:1-13 https://doi:10.12103/j.issn.2096-2355.2020.03.001
14. Ferrer A, Pal L, Hubbe M (2017) Nanocellulose in packaging: Advances in barrier layer technologies Ind Crop Prod 95:574-582 https://doi:10.1016/j.indcrop.2016.11.012
15. He Y, Zhang X, Chen W, Zhang B, Zhang Z (2019) Experimental study and thermal analysis of the combustion characteristics of powder-activated cokes Powder Technol 356:640-648 https://doi:10.1016/j.powtec.2019.08.084
16. Huang X, Li R, Zeng L, Li X, Xi Z, Wang K, Li Y (2020) A multifunctional carbon nanotube reinforced nanocomposite modified via soy protein isolate: A study on dispersion, electrical and mechanical properties Carbon 161:350-358 https://doi:10.1016/j.carbon.2020.01.069
17. Kalashnikova I, Bizot H, Cathala B, Capron I (2012) Modulation of cellulose nanocrystals amphiphilic properties to stabilize oil/water interface Biomacromolecules 13:267-275 https://doi:10.1021/bm201599j
18. Karinkanta P, Illikainen M, Niinimäki J (2014) Effect of different impact events in fine grinding mills on the development of the physical properties of dried Norway spruce (Picea abies) wood in pulverisation Powder Technol 253:352-359 https://doi:10.1016/j.powtec.2013.11.044
19. Laitinen O, Ojala J, Sirviö JA, Liimatainen H (2017a) Sustainable stabilization of oil in water emulsions by cellulose nanocrystals synthesized from deep eutectic solvents Cellulose 24:1679-1689 https://doi:10.1007/s10570-017-1226-9
20. Laitinen O, Suopajarvi T, Osterberg M, Liimatainen H (2017b) Hydrophobic, superabsorbing aerogels from choline chloride-based deep eutectic solvent pretreated and silylated cellulose nanofibrils for selective oil removal ACS Appl Mater Interfaces 9:25029-25037 https://doi:10.1021/acsami.7b06304
21. Li P, Sirvio JA, Asante B, Liimatainen H (2018) Recyclable deep eutectic solvent for the production of cationic nanocelluloses Carbohydr Polym 199:219-227 https://doi:10.1016/j.carbpol.2018.07.024
22. Li P, Sirvio JA, Haapala A, Liimatainen H (2017) Cellulose nanofibrils from nonderivatizing urea-based deep eutectic solvent pretreatments ACS Appl Mater Interfaces 9:2846-2855 https://doi:10.1021/acsami.6b13625
23. Ling Z, Edwards JV, Guo Z, Prevost NT, Nam S, Wu Q, French AD, Xu F (2018) Structural variations of cotton cellulose nanocrystals from deep eutectic solvent treatment: Micro and nano scale Cellulose 26:861-876 https://doi:10.1007/s10570-018-2092-9
24. Liu C, Li B, Du H, Lv D, Zhang Y, Yu G, Mu X, Peng H (2016) Properties of nanocellulose isolated from corncob residue using sulfuric acid, formic acid, oxidative and mechanical methods Carbohydr Polym 151:716-724 https://doi:10.1016/j.carbpol.2016.06.025
25. Liu Y, Chen W, Xia Q, Guo B, Wang Q, Liu S, Liu Y, Li J, Yu H (2017) Efficient cleavage of lignin-carbohydrate complexes and ultrafast extraction of lignin oligomers from wood biomass by microwave-assisted treatment with deep eutectic solvent ChemSusChem 10:1692-1700 https://doi:10.1002/cssc.201601795

26. Loow Y-L, New EK, Yang GH, Ang LY, Foo LYW, Wu TY (2017) Potential use of deep eutectic solvents to facilitate lignocellulosic biomass utilization and conversion Cellulose 24:3591-3618 https://doi:10.1007/s10570-017-1358-y
27. Lv D, Du H, Che X, Wu M, Zhang Y, Liu C, Nie S, Zhang X, Li B (2019) Tailored and integrated production of functional cellulose nanocrystals and cellulose nanofibrils via sustainable formic acid hydrolysis: Kinetic study and characterization ACS Sustain Chem Eng 7:9449-9463 https://doi:10.1021/acssuschemeng.9b00714
28. Lynam JG, Kumar N, Wong MJ (2017) Deep eutectic solvents' ability to solubilize lignin, cellulose, and hemicellulose; thermal stability; and density Bioresour Technol 238:684-689 https://doi:10.1016/j.biortech.2017.04.079
29. Man Z, Muhammad N, Sarwono A, Bustam MA, Vignesh Kumar M, Rafiq S (2011) Preparation of cellulose nanocrystals using an ionic liquid J Polym Environ 19:726-731 https://doi:10.1007/s10924-011-0323-3
30. Morris ER, Cutler AN, Ross-Murphy SB, Rees DA, Price J (1981) Concentration and shear rate dependence of viscosity in random coil polysaccharide solutions Carbohydr Polym 1:5-21 https://doi:10.1016/0144-8617(81)90011-4
31. Nishiyama Y (2009) Structure and properties of the cellulose microfibril J Wood Sci 55:241-249 https://doi:10.1007/s10086-009-1029-1
32. Novo LP, Bras J, Garcia A, Belgacem MN, Curvelo AAS (2015) Subcritical water: A method for green production of cellulose nanocrystals ACS Sustain Chem Eng 3:2839–2846 https://doi:10.1021/acssuschemeng.5b00762
33. Pääkkö M, Ankerfors M, Kosonen H, Nykänen A, Ahola S, Österberg M, Ruokolainen J, Laine J, Larsson PT, Ikkala O, Lindström T (2007) Enzymatic hydrolysis combined with mechanical shearing and high-pressure homogenization for nanoscale cellulose fibrils and strong gels Biomacromolecules 8:1934-1941 https://doi:10.1021/bm061215p
34. Piras CC, Fernández-Prieto S, De Borggraeve WM (2019) Ball milling: A green technology for the preparation and functionalisation of nanocellulose derivatives Nanoscale Advances 1:937-947 https://doi:10.1039/c8na00238j
35. Pires JRA, Souza VGL, Fernando AL (2019) Valorization of energy crops as a source for nanocellulose production – current knowledge and future prospects Ind Crop Prod 140:111642-111659 https://doi:10.1016/j.indcrop.2019.111642
36. Selkala T, Sirvio JA, Lorite GS, Liimatainen H (2016) Anionically stabilized cellulose nanofibrils through succinylation pretreatment in urea-lithium chloride deep eutectic solvent ChemSusChem 9:3074-3083 https://doi:10.1002/cssc.201600903
37. Seta FT, An X, Liu L, Zhang H, Yang J, Zhang W, Nie S, Yao S, Cao H, Xu Q, Bu Y, Liu H (2020) Preparation and characterization of high yield cellulose nanocrystals (CNC) derived from ball mill pretreatment and maleic acid hydrolysis Carbohydr Polym 234:115942-115951 https://doi:10.1016/j.carbpol.2020.115942

38. Silva GG, Couturier M, Berrin JG, Buleon A, Rouau X (2012) Effects of grinding processes on enzymatic degradation of wheat straw Bioresour Technol 103:192-200 https://doi:10.1016/j.biortech.2011.09.073
39. Sirviö JA, Ukkola J, Liimatainen H (2019) Direct sulfation of cellulose fibers using a reactive deep eutectic solvent to produce highly charged cellulose nanofibers Cellulose 26:2303-2316 https://doi:10.1007/s10570-019-02257-8
40. Sirviö JA, Visanko M (2017) Anionic wood nanofibers produced from unbleached mechanical pulp by highly efficient chemical modification J Mater Chem A 5:21828-21835 https://doi:10.1039/c7ta05668k
41. Sirvio JA (2018) Cationization of lignocellulosic fibers with betaine in deep eutectic solvent: Facile route to charge stabilized cellulose and wood nanofibers Carbohydr Polym 198:34-40 https://doi:10.1016/j.carbpol.2018.06.051
42. Sirvio JA, Visanko M, Liimatainen H (2016) Acidic deep eutectic solvents as hydrolytic media for cellulose nanocrystal production Biomacromolecules 17:3025-3032 https://doi:10.1021/acs.biomac.6b00910
43. Suopajarvi T, Sirvio JA, Liimatainen H (2017) Nanofibrillation of deep eutectic solvent-treated paper and board cellulose pulps Carbohydr Polym 169:167-175 https://doi:10.1016/j.carbpol.2017.04.009
44. Tang LR, Huang B, Ou W, Chen XR, Chen YD (2011) Manufacture of cellulose nanocrystals by cation exchange resin-catalyzed hydrolysis of cellulose Bioresour Technol 102:10973-10980 https://doi:10.1016/j.biortech.2011.09.070
45. Tenhunen T-M, Lewandowska AE, Orelma H, Johansson L-S, Virtanen T, Harlin A, Österberg M, Eichhorn SJ, Tammelin T (2017) Understanding the interactions of cellulose fibres and deep eutectic solvent of choline chloride and urea Cellulose 25:137-150 https://doi:10.1007/s10570-017-1587-0
46. Tenhunen TM, Hakalahti, M., Kouko, J., Salminen, A., Härkäsalmi, T., Pere, J., Harlin, A., and Hänninen, T. (2016) Method for forming pulp fibre yarns developed by a design-driven process BioResources 11: 2492-2503 https://doi:10.15376/biores.11.1.2492-2503
47. Tomé LIN, Baião V, da Silva W, Brett CMA (2018) Deep eutectic solvents for the production and application of new materials Applied Materials Today 10:30-50 https://doi:10.1016/j.apmt.2017.11.005
48. Wang N, Ding E, Cheng R (2007) Thermal degradation behaviors of spherical cellulose nanocrystals with sulfate groups Polymer 48:3486-3493 https://doi:10.1016/j.polymer.2007.03.062
49. Wang R, Chen L, Zhu JY, Yang R (2017) Tailored and integrated production of carboxylated cellulose nanocrystals (CNC) with nanofibrils (CNF) through maleic acid hydrolysis ChemNanoMat 3:328-335 https://doi:10.1002/cnma.201700015
50. Wu M, Sukyai P, Lv D, Zhang F, Wang P, Liu C, Li B (2020) Water and humidity-induced shape memory cellulose nanopaper with quick response, excellent wet strength and folding resistance Chemical Engineering Journal 392:123673-123683 https://doi:10.1016/j.cej.2019.123673

51. Yang X, Biswas SK, Han J, Tanpichai S, Li MC, Chen C, Zhu S, Das AK, Yano H (2021) Surface and interface engineering for nanocellulosic advanced materials Adv Mater:2002264-2002293 https://doi:10.1002/adma.202002264
52. Yang X, Xie H, Du H, Zhang X, Zou Z, Zou Y, Liu W, Lan H, Zhang X, Si C (2019) Facile extraction of thermally stable and dispersible cellulose nanocrystals with high yield via a green and recyclable FeCl3-catalyzed deep eutectic solvent system ACS Sustain Chem Eng 7:7200-7208 https://doi:10.1021/acssuschemeng.9b00209
53. Yu W, Wang C, Yi Y, Zhou W, Wang H, Yang Y, Tan Z (2019) Choline chloride-based deep eutectic solvent systems as a pretreatment for nanofibrillation of ramie fibers Cellulose 26:3069-3082 https://doi:10.1007/s10570-019-02290-7
54. Zhang L, Tsuzuki T, Wang X (2015) Preparation of cellulose nanofiber from softwood pulp by ball milling Cellulose 22:1729-1741 https://doi:10.1007/s10570-015-0582-6
55. Zhang Q, Benoit M, De Oliveira Vigier K, Barrault J, Jerome F (2012) Green and inexpensive choline-derived solvents for cellulose decrystallization Chemistry 18:1043-1049 https://doi:10.1002/chem.201103271
56. Zhang Y, Wang J, Liu C, Liu Y, Li Y, Wu M, Li Z, Li B (2021) Influence of drying methods on the structure and properties of cellulose formate and its application as a reducing agent Int J Biol Macromol 170:397-405 https://doi:10.1016/j.ijbiomac.2020.12.185

Figures

Figure 1

Integrated preparation route of NC samples via DES pretreatment and the followed ball milling

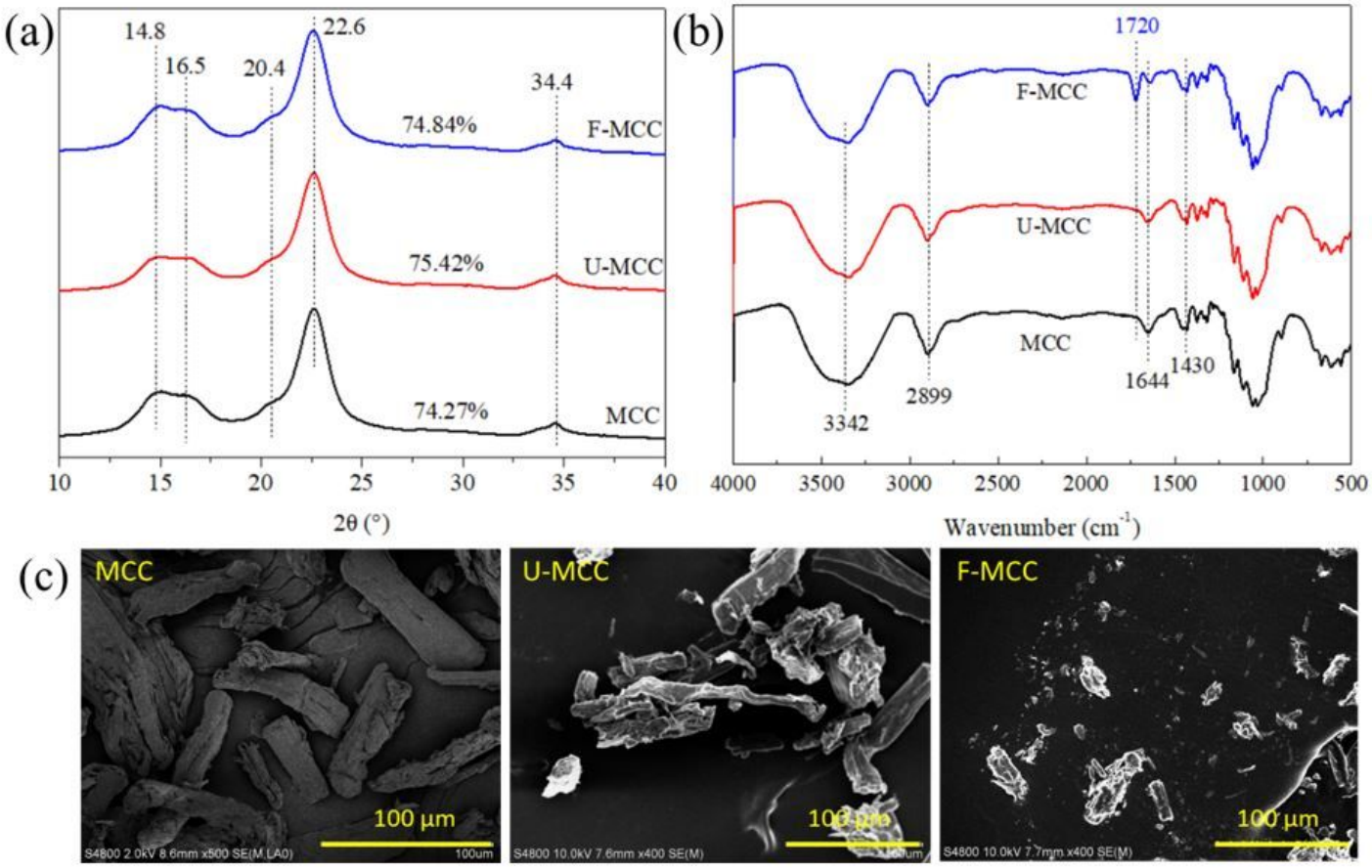

Figure 2

XRD patterns (a), FTIR spectra (b), and SEM images of MCC (c) before and after DES pretreatment for 2 h

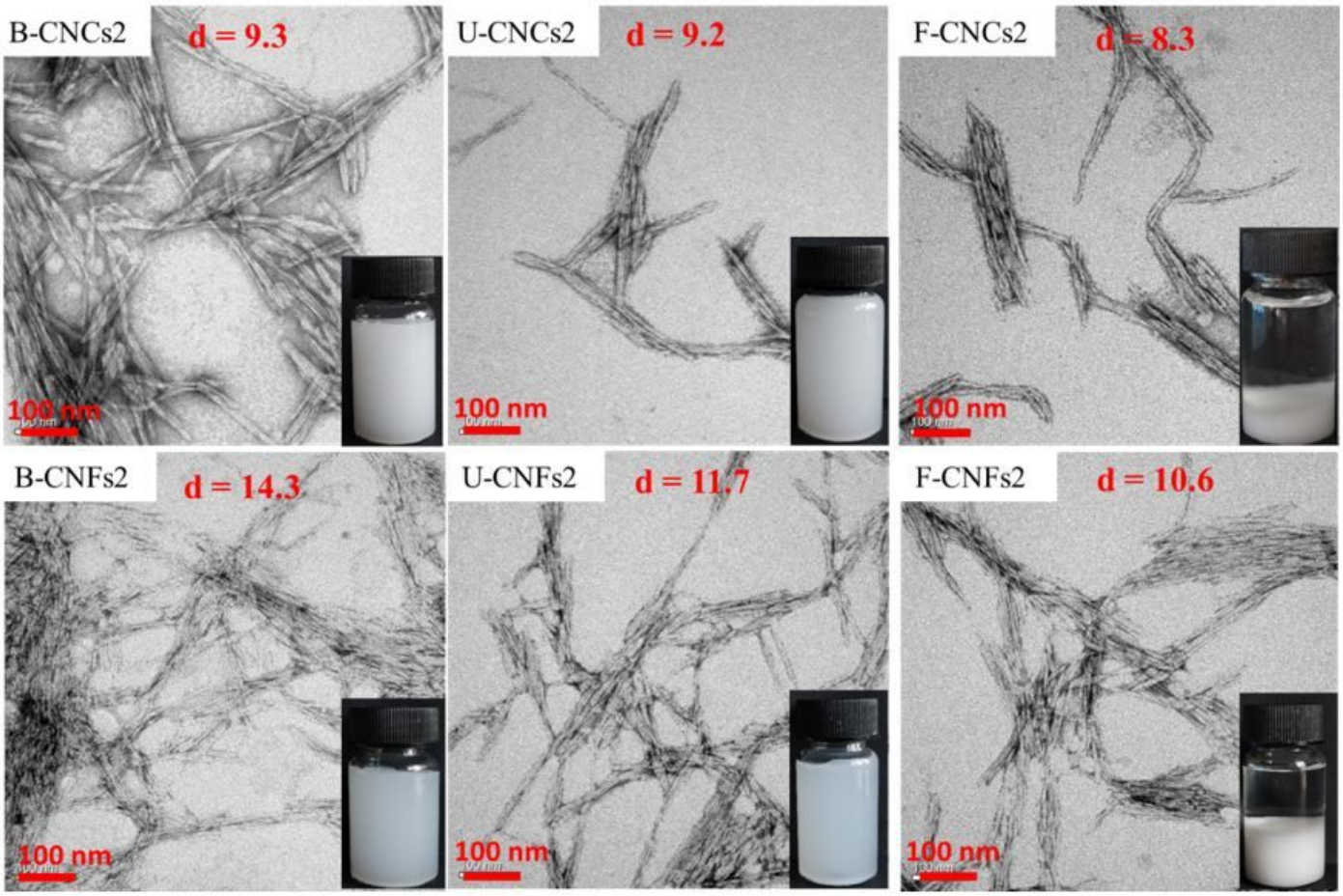

Figure 3

TEM images and mean diameter (d) of the CNCs and CNFs separated from B-NC2, F-NC2 and U-NC2 with the ball milling for 16 h (The digital images on the bottom-right corner show CNCs or CNFs suspension in water (0.1 wt%) after standing for 24 h)

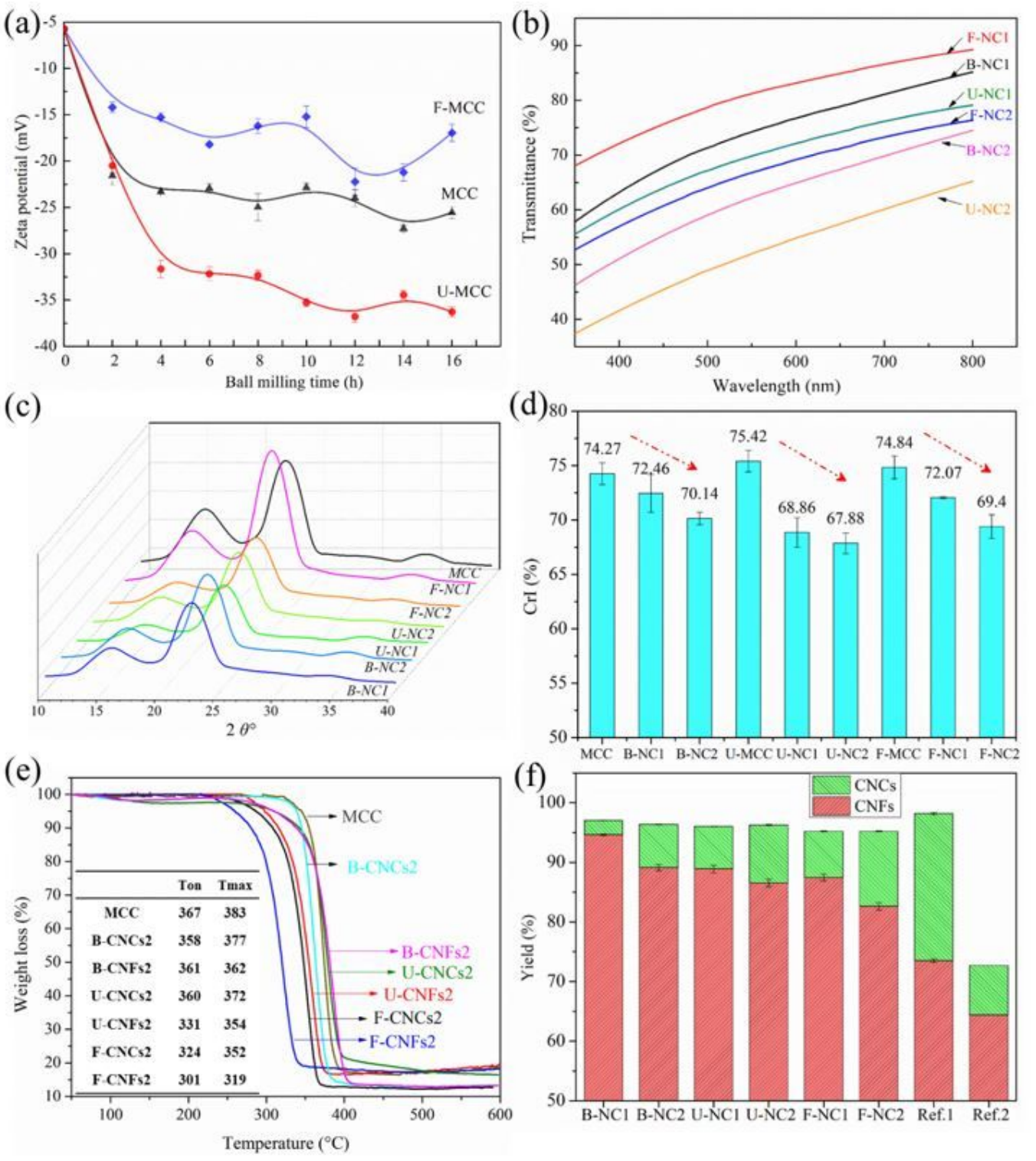

Figure 4

(a) Zeta potential of MCC samples after ball milling. (b) Transmittances of NC dispersions. XRD patterns (c) and the crystallinity index (d) of NC samples. (e) TG curves of NC samples. (f) Yield of CNCs and CNFs in NC samples, the results of Ref. 1 (Suopajarvi et al. 2017) and 2 (Wang et al. 2017) were used for comparison

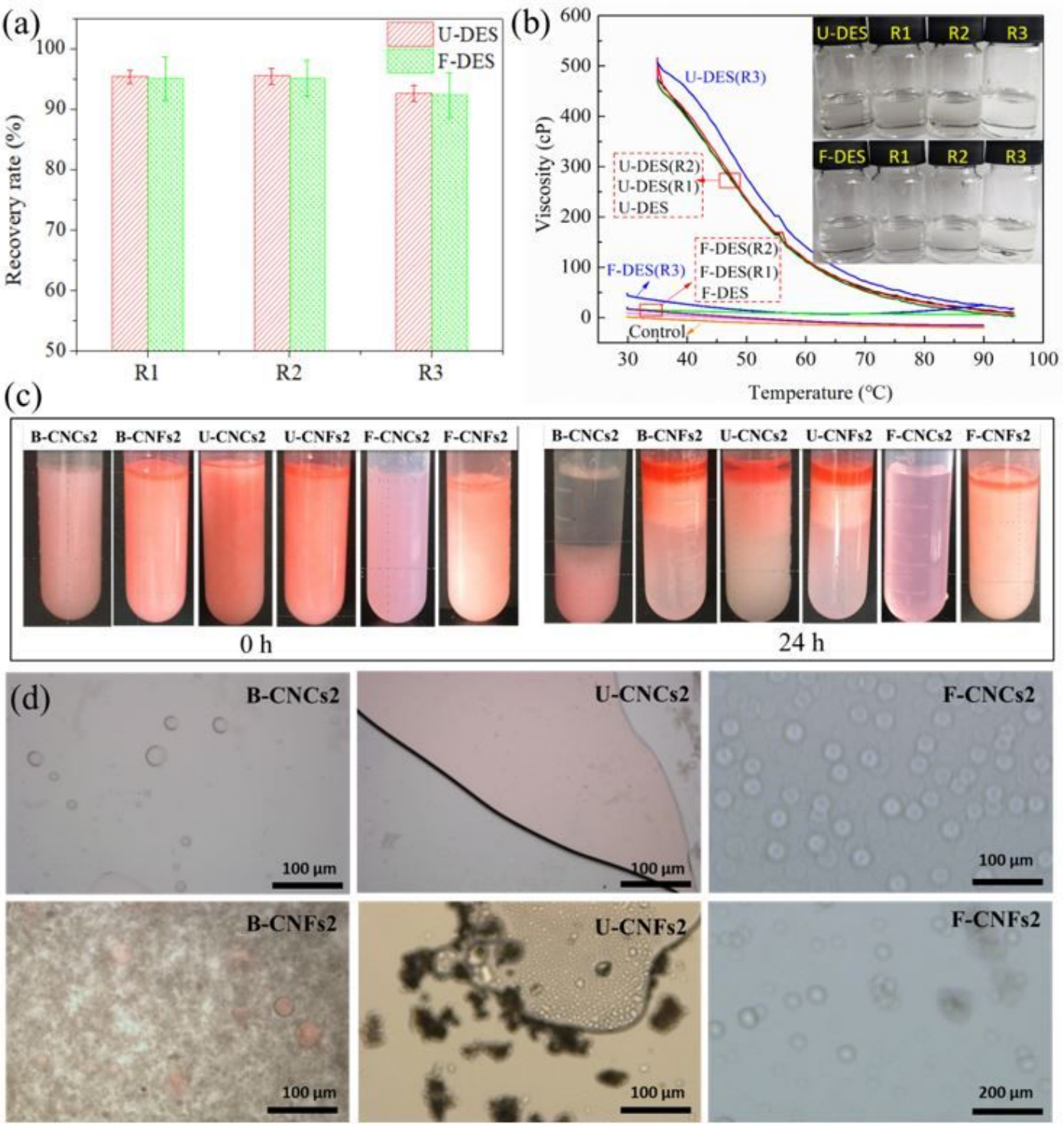

Figure 5

(a) Recovery rate of DES after different cycle. (b) Viscosity of the recycled DES after different cycle (R1, R2 and R3 are the cycle numbers of the DES). Digital photos (c) and microphotographs (d) of the oil/water mixture containing 0.2 wt% CNCs or CNFs samples

Supplementary Files

This is a list of supplementary files associated with this preprint. Click to download.

- Graphicabstract.tif
- Supportinginformation20210613.docx